

# Effects of different indentation methods on fatigue life extension of cracked specimens

S.M.J. Razavi<sup>1</sup>, M.R. Ayatollahi<sup>1\*</sup>, A. Amouzadi<sup>1</sup>, F. Berto<sup>2</sup>

<sup>1</sup> *Fatigue and Fracture Lab., Center of Excellence in Experimental Solid Mechanics and Dynamics, School of Mechanical Engineering, Iran University of Science and Technology, Narmak, 16846, Tehran, Iran.*

<sup>2</sup> *Department of Mechanical and Industrial Engineering, Norwegian University of Science and Technology (NTNU), Richard Birkelands vei 2b, 7491 Trondheim, Norway.*

## Abstract

In this paper, three different indentation methods have been investigated for crack arresting and fatigue life enhancement of cracked components. The influence of residual stresses induced by indentation on fatigue crack growth (FCG) rate was explored by experiments and numerical simulations. Fatigue tests were conducted on a group of specimens which were indented on the crack tip by various indentation load magnitudes. For another group of specimens, the double indentation and triple indentation methods were applied on the cracked specimens with the aim of obtaining proper residual stress fields that contribute to higher crack growth retardations. Both the numerical and experimental results revealed that the higher indentation loads led to larger domain of compressive residual stress around the crack tip and consequently to higher fatigue life extension. In addition, the triple indentation method resulted in more FCG retardation compared to single and double indentation methods. Furthermore, for the specimens repaired by double and triple indentation methods, indenting ahead of the crack tip led to retardation in more crack growth compared to the other horizontal positions of indentation.

*Keywords:* fatigue crack growth, crack retardation, residual stress distribution, elasto-plastic indentation, fatigue damage repair.

## 1. Introduction

Cracks are very often generated in mechanical components during their service lives and/or their manufacturing processes. Under cyclic loading, cracks may gradually propagate until final failure of the cracked element. Hence, several methods have been proposed by researchers to extend the fatigue life in the cracked components that cannot be replaced as soon as the crack is observed; this situation commonly happens when the replacement of new parts are time consuming and costly. Different techniques are utilized for arresting or retarding fatigue crack propagation, for example, crack removal and welding<sup>1,2</sup>, crack filling<sup>3-5</sup>, application of composite patches on the cracked area<sup>6</sup>, drilling stop-holes in the vicinity of the crack tip<sup>7-11</sup> and applying the residual compressive stresses in the vicinity of crack in order to reduce the intensified stress field at the crack tip. The residual compressive stresses can be generated through overloading<sup>12-14</sup>, laser shock peening<sup>15-17</sup>, shot peening<sup>18-20</sup> and spot heating<sup>21-23</sup>.

---

\* Corresponding author: M.R. Ayatollahi, Email: m.ayat@iust.ac.ir, Phone: +98-21-77240201

In addition to the above-mentioned fatigue crack retardation methods, the indentation technique can be used for cracked components under fatigue loading. This technique utilizes a compressive force applied by an indenter in order to induce residual compressive stresses around the crack tip. Three major indentation methods can be considered for fatigue life extension, including the single indentation at the crack tip (see Fig. 1a), double indentation on both sides of the expected crack path (see Fig. 1b), and triple indentation (i.e. one indentation at crack tip and two symmetric indentations at both sides of the crack path) (see Fig. 1c). **The single indentation is used to reduce the stress singularity at the crack tip, to reduce the stress intensity factor, and hence to retard the FCG<sup>24</sup>.** Indenting two regions symmetric relative to the crack line is the other method to decrease the crack growth rate and to increase the fatigue life of the cracked part. The triple indentation method which is introduced in this paper is a combination of the single and double indentation methods.

The single and double indentation methods have been investigated in very few papers. A number of researchers investigated the parameters that affect the single and double indentation methods for example Goto et al.<sup>24</sup> studied the concurrent effects of stop-hole and indentation on the arrest of FCG. Their results showed that drilling stop-holes in the vicinity of crack tip increased the FCG life about three times while the effect of an indentation was considerably more remarkable. According to the experiments conducted by Goto et al., by using indentation at stresses above the fatigue limit, up to about 50 times increase in the FCG life was obtained. Ruzek et al.<sup>25</sup> showed that crack growth retardation can be induced by applying mechanical impact in front of the crack tip. They also investigated numerically the effects of impact energy, crack length and load level on the FCG retardation. In a paper by Song and Sheu<sup>26</sup>, the magnitude of indentation loads applied on both sides of the expected crack path was changed and its effect on the crack retardation development was evaluated. By applying 3-10 kN indentation loads using a hemispherical indenter, their results revealed that stronger crack closure effects and better growth retardations can be achieved when higher indentation loads were applied. Lim et al.<sup>27</sup> proposed a new geometry for the indenter namely the ring indenter and tested a number of single edge crack specimens repaired by the proposed indenter under fatigue loading. According to their experimental results, the compressive residual stresses induced inside the ring-shape indentation area improved the total fatigue life of the tested samples.

As mentioned above, all the previous researches on indentation technique are limited only to simple cases of single and double indentations. The aim of this paper is twofold: first to study the effects of geometry and loading parameters on the performance of single and double indentation methods, second to investigate the efficiency of triple indentation method on the life enhancement of cracked specimens under fatigue loading in comparison with single or double indentation methods. The indentation load level and the horizontal positions of indentation relative to the crack tip are considered as the main variables in both numerical and experimental studies. The effect of indentation on stress variation along

the crack path, crack growth rate and fatigue life are evaluated numerically and experimentally and proper locations for indentations with maximum fatigue life improvement are determined.

## 2. Experimental procedures

For conducting fatigue tests, compact tension (CT) specimens were fabricated from aluminum alloy 7075-T6 with a thickness of 5 mm and width of 60 mm. The CT specimens were all made in the L–T orientation i.e. the crack propagation was in the transverse direction relative to the rolling direction. The dimensions of specimens and the locations of indentation are illustrated in Fig. 2, where  $V$  and  $H$  are vertical and horizontal positions of indentation center with respect to the crack tip. The stress-strain curve of the material obtained from tensile test according to ASTM E8/E8M is shown in Fig. 3. The mechanical properties of aluminum alloy 7075-T6 are presented in Table 1. All the specimens were fabricated using a milling machine; besides CNC wire cut machine was employed for creating the initial notches of length 34 mm. Indentation load level and the horizontal position of indentation were the two variable parameters investigated in the experiments.

The specimens were tested under constant amplitude axial fatigue loading, using a closed-loop servo-hydraulic testing machine with a sinusoidal waveform loading at a frequency of 10 Hz. The stress ratio  $R$  was 0.1 and the maximum load of  $F_{app} = 1.3$  kN was applied to all specimens. A pre-crack of length  $a_0 = 4$  mm was created in each specimen by fatigue loading and then a hemispherical indenter with 5 mm diameter was employed for making indentations on one side of each CT specimen (see Fig. 4). The specimen was under-pinned by a thick plate, then the indenter was pressed in front of the crack tip. The practical process of applying the single indentation method at the crack tip has been well described in references [24,25,27]. Such procedures often include a preparation stage for crack tip detection using appropriate non-destructive testing (NDT) techniques. The same NDT methods can also be used for the double and triple indentation methods to find the crack geometry. Once the crack geometry is found, the locations of the indentation centers on both sides of the crack line can be specified. According to the small thickness of the CT specimens compared to the other dimensions, there is a chance of distortion and buckling of samples during the tensile test. In order to prevent buckling of the specimens during the loading process, four anti-buckling plates were used on both sides of CT specimens. Fig. 5 illustrates the configuration of anti-buckling plates. Four steel plates were placed on both sides of CT specimens which were fastened by screws. The fatigue test set up is illustrated in Fig. 6. Three samples for each specimen configuration were manufactured and tested.

Three sets of experiments were performed: single indentation, double indentation and triple indentation. In the first set of fatigue tests, three different indentation loads of  $F_{ind} = 1, 1.75$  and  $2.5$  kN were applied just ahead of the crack tip to study the influence of indentation load level on the FCG retardation of CT

specimens when single indentation method is employed. For the second set of fatigue tests, in order to investigate the influence of horizontal location of double indentations, symmetric double indentations with a fixed indentation load level of  $F_{\text{ind}} = 2.5$  kN, were applied in three different horizontal positions of indentation centers relative to the crack tip ( $H = -2, 0, 2$  mm) and a constant vertical distance of  $V = 2$  mm (see Fig. 2). A combination of single and double indentations was employed for the third set of specimens repaired by the triple indentation method. After applying the indentation loads, the indented specimens were subjected to cyclic loading and the incremental FCG life was recorded for every 1 mm segment of FCG. A digital camera (Canon EOS 600D with an EF 100 mm f/2.8 Macro Lens, Tokyo-Japan) was used to track the fatigue crack growth at 5 s intervals during testing so that the fatigue crack growth life-crack length ( $N-a$ ) data could be generated. The cyclic loading was interrupted when the crack length reached from the initial length of 4 mm to the value of  $a = 12$  mm.

### 3. Finite element simulation

The numerical evaluation of indentation effect on the stress distribution along the crack growth path was conducted by a set of three-dimensional finite element (FE) analyses using ABAQUS software. The FE model was consisted of two parts, a rigid shell as the hemispherical indenter of 5 mm diameter and one deformable part with elasto-plastic material behavior representing the CT specimen with the dimensions of  $62.5 \times 60 \times 5$  mm and a pre-crack of length  $a_0 = 4$  mm. The specimen was simulated according to the mechanical properties listed in Table 1 using 20-node quadratic brick elements. A mesh convergence study was also undertaken to ensure that a proper number of elements was used in finite element analysis. The discretized model is shown in Fig. 7. With the aim of improving the accuracy of the results, higher mesh density was used near the crack tip. FE simulations were conducted in three general steps including:

- (1) Indentation process: applying appropriate indentation loads ( $F_{\text{ind}}$ ) on the model of CT specimen.
- (2) Removing the indenter from the specimen surface.
- (3) Application of crack opening load i.e. the maximum load applied in the axial fatigue test  $F_{\text{app}} = 1.3$  kN, on the CT specimen.

During the first two steps, the bottom surface of CT specimen was fixed normal to its plane. Before step 3 i.e. at the end of step 2, this boundary condition was deactivated. As the output of analysis, the stress field near the crack tip on the indented surface was recorded before and after applying the opening force. The contact between the indenter model and the CT specimen model was defined using the penalty contact method. Fig. 8. illustrates a typical contour map of residual out-of-plane stress near the crack tip for the FE model indented on the crack tip by  $F_{\text{ind}} = 1$  kN load level.

### 4. Results and discussions

Two investigated variable parameters are the indentation load level and the indentation position with respect to the crack tip. The results related to each indentation method are described and discussed in this section.

#### *4.1. Single indentation method*

The indentation method is based on applying external loads that produce localized inelastic deformation. Upon removal of the external loading, both tensile and compressive stresses are induced in the specimen in order to satisfy all equations of internal force and moment equilibrium. The distribution of these residual stresses and their magnitude play the key role in improvement of fatigue resistance. The favorite residual stress field resulted by indentation can be obtained if the compressive part of the stress distribution occurs in front of the crack tip and along the expected path of crack growth. Fig. 9 illustrates the variations of stress perpendicular to the crack plane ( $\sigma_y$ ) along the expected crack growth path, before and after applying the opening force. The indentation load level controls the distance ahead of the crack tip which is under the influence of compressive residual stress. According to Fig. 9a, higher indentation loads led to larger zones of compressive residual stress. There is a tensile residual stress field right after the compressive field which may increase the FCG rate. After applying the opening force, the remaining compressive stress level ahead of the crack tip is proportional to the indentation load level (see Fig. 9b). The numerical results show that, an increase in the indentation load rises the value of compressive residual stresses in front of the crack tip.

The variations of experimental FCG rates ( $da/dN$ ) in the CT specimens indented with different indentation loads, are illustrated in Fig. 10. Before the indentation process, FCG rate had a constant slope. But, exactly at the pre-crack length, the indentation caused a sudden reduction of the FCG rate. Higher indentation loads resulted in more reduction in the FCG rate. The minimum crack growth rate is related to the indentation load value of 2.5 kN. As it can be seen from Fig. 9, the tensile residual stress next to the compressive field resulted in higher FCG rates after the indentation region compared with the plain specimens. However, the reduction of FCG rate is much higher than its increase due to the tensile residual stresses. The details of fatigue tests performed on the CT specimens repaired by single indentation are provided in Table 2.

Fig. 11 shows the experimental fatigue lives of specimens which were indented on the crack tip by various indentation load levels. Up to the pre-crack size of 4 mm, the curves for all specimens are coincided, however, for larger crack lengths, there is a sudden increase in the fatigue life for the indented specimens. The FCG life improvement for the indentation loads of  $F_{ind} = 1, 1.75$  and 2.5 kN were about 33%, 67% and 143% compared to the plain specimen. Additionally, a strong dependency on the indentation load can be observed that reveals the influence of magnitude of compressive residual stress

(see Table 2). According to the experimental results, it can be concluded that the majority of fatigue life in the indented specimens is nearly controlled by the FCG life up to  $a - a_0 = 1$  mm.

#### 4.2. Double indentation method

Selecting appropriate positions for indentation is of great importance. In order to determine the proper positions for double indentation, three different horizontal indentation positions of  $H = -2, 0$  and  $2$  mm were considered in FE simulation. Fig. 12 displays the distribution of Y axis residual stress  $\sigma_y$  around the crack tip for these three positions.

Fig.13 shows the variations of crack opening stress  $\sigma_y$  at the end of second step (i.e. after removing the indenter and before applying the opening force), along the expected crack growth path as exported from the FE model. According to Fig. 13a, 104% larger length in front of the crack tip is influenced by the compressive stress which is induced by double indentation in the positive horizontal position of  $H = 2$  mm in comparison with the horizontal position of  $H = 0$ , hence more FCG lives are obtained for the case of  $H = 2$  mm. During FCG, the compressive residual stress ahead of the crack tip slightly decreases and gradually tends to zero, but its tendency to zero occurs in larger distance from the crack tip in the horizontal position of  $H = 2$  mm, which evidently causes higher retardation in fatigue crack propagation.

According to Fig. 13a, only compressive residual stresses are available along the FCG path. It is worth mentioning that this compressive residual stress  $\sigma_{y/compressive}$  was surrounded by tensile residual stresses  $\sigma_{y/tensile}$  on the indented surface in the far field to have the stress equilibrium. Comparing the residual stress variations for the single indentation (Fig. 9a) and double indentation (Fig. 13a) methods reveals that lack of tensile residual stresses in the specimens repaired by double indentation method has intensified the FCG retardation for the cases of  $H = 0$  and  $2$  mm. As it is illustrated in Fig. 13b, after applying the opening force, the compressive residual stress ahead of the crack tip is also dependent on the indentation position, the maximum compressive stress corresponds to the model which was indented in positive horizontal position ( $H = 2$  mm).

Fig. 14 presents the variation of FCG rate versus the crack length. Due to the presence of compressive residual stress field at both sides of crack line, a sudden decrease occurs in FCG rate after indenting the CT specimen. The decrease is proportional to the indentation position. The FCG lives of the specimens repaired by double indentations in different horizontal distances from the crack tip are shown in Fig. 15. Since indentations ahead of the crack tip is more capable of reducing the stress singularity at the crack tip (Fig. 13b), the maximum FCG retardation is observed for the specimen with positive indentation position ( $H = 2$  mm) (see Fig. 14). In this case, the specimen is indented on the expected crack growth sector and hence a larger length of crack growth path is under the influence of indentation residual stress field. Indenting the CT specimens in horizontal positions of  $H = -2, 0$  and  $2$  mm provides 37%, 167% and 265% fatigue life enhancement, respectively. In all cases, when the crack tip passes the compressive residual

stress field induced by indentation, the crack extends with higher rates. Therefore, the FCG rates of different repaired specimens have roughly equal values for larger crack lengths. The details of FCG lives of double indentation specimens are provided in Table 3.

#### *4.3. Triple indentation method*

As previously mentioned, the single indentation method provides considerable compressive residual stress at crack tip followed by a tensile residual stress (Fig. 9a). However, the double indentation method induces pure compressive residual stress along the FCG path with lower compressive stresses compared to single indentation method (Fig. 13a). In this section, these two indentation methods are combined and the triple indentation method is suggested in order to provide a high level of compressive residual stresses around the crack tip followed by a lower tensile residual stress field. According to the triple indentation method, one indentation is performed on the crack tip and two indentations are also performed symmetrically on both sides of the crack line in three different horizontal indentation positions of  $H = -2, 0$  and  $2$  mm. Fig. 16 shows the Y axis residual stress distribution  $\sigma_y$  around the crack tip obtained from FE analyses.

The variations of residual stress perpendicular to the crack plane  $\sigma_y$  at the end of second step (after the indentation process and before applying the opening force), are shown in Fig. 17 along the expected crack growth path for different horizontal indentation positions. According to Fig. 17a, the triple indentation method takes the advantages of both single and double indentation methods such that higher levels of compressive residual stress around the crack tip in addition to larger areas of residual stress field are observed in FE models of CT specimens repaired by triple indentations. According to FE results, a larger distance ahead of crack tip is influenced by the compressive residual stresses in the positive horizontal position of  $H = 2$  mm in comparison to the other horizontal positions, therefore more FCG lives are obtained for the case of  $H = 2$  mm. According to Fig. 17b, after applying the opening force, the compressive residual stresses along the expected path of crack growth depend also on the indentation position. In addition, the maximum effective length of compressive residual stress corresponds to the model which is indented in the positive horizontal position ( $H = 2$  mm).

The variations of FCG rate and FCG lives for specimens with triple indentation are shown in Figs. 18 and 19, respectively. Similar to other indentation methods, a sudden FCG rate reduction occurs after indenting the CT specimens. The amount of FCG rate reduction depends on the indentation position and the highest FCG rate reduction takes place in the specimens indented at  $H = 2$  mm resulting in the maximum FCG retardation in these specimens (see Fig. 19). By indenting the crack tip and the two sides of crack line in the CT specimens, 153%, 184% and 435% FCG life enhancement could be achieved for the specimens indented in horizontal positions of  $H = -2, 0$  and  $2$  mm, respectively. The details of FCG lives of triple indented specimens are presented in Table 4.

#### 4.4. Observation of microstructure around the indentation area

The fracture surface of specimens after fatigue failure was studied via scanning electron microscopy (SEM). Fig. 20 displays the micro-morphologies of stable crack growth zone both for a plain specimen and for the single, double and triple indented specimens with an indentation load of  $F_{ind} = 2.5$  kN. The observed locations in the SEM photos are 5 mm away from the edge of notch (or 1 mm away from the indentation position). Magnified previews of images shown in Fig. 20 are presented in Fig. 21. The fatigue crack growth direction in Figs. 20 and 21 is horizontal and from right to left. The wave pattern strips on the fracture surface of both repaired and plain specimens are the fatigue striations which largely exist in the fracture surface of the tested specimens. According to Fig. 20, more continuous fatigue striations can be observed on the fracture surface of the indented specimens (Fig. 20 b,c,d) resulting in a more stable crack propagation through the indented region. According to Fig. 21, the parallel lines are the main micro-characteristic of fatigue crack growth with a direction perpendicular to the FCG direction. Decreased distances between the parallel lines represent reduction in the FCG rate and consequently, enhancement in the fatigue life of specimen. As shown in Fig. 21, all the indented specimens have lower spacing between the fatigue striations compared to the plain specimen. Therefore, the crack growth rates in the indented specimens are lower than that of the plain specimen, which are in accordance with the observations described in Sections 3.1 to 3.3.

As mentioned before, all the indentations in this research were only performed on one side of the cracked specimen which is suitable for repairing the components which can be accessed only on one side. It is expected to have higher fatigue retardations for indentation on both sides of the crack due to higher residual stresses around the crack tip. It is finally noted that although the vertical distance of crack flank indentation was considered to be constant in this research, further studies can be conducted using various vertical distances of indentation in order to assess its effect on FCG rate. Even though the reported results in this paper are obtained for the CT specimens made of 7075-T6 aluminum alloy, the same approaches can be developed to extend the FCG life of other cracked specimens.

## 5. Conclusions

The effects of indentation load level and position of indentation on fatigue life extension of CT specimens made of 7075-T6 aluminum alloy were investigated both experimentally and numerically. Three different methods of indentation namely the single indentation method (at the crack tip), the double indentation method (at crack flanks) and the triple indentation method (at the crack tip and crack flanks) were evaluated. For the indented specimens, the stress concentration at the crack tip was affected by the residual stress field induced by indentation. According to the results, by increasing the indentation load level, more crack growth retardation and consequently higher fatigue lives were obtained. The fatigue life



improvements for the specimens indented at the crack tip with indentation load levels of 1 kN, 1.75 kN and 2.5 kN were 33%, 67% and 143%, respectively.

The effect of location of double and triple indentations on fatigue lives of specimens was investigated by considering three horizontal positions of indentation with respect to the crack tip ( $H = -2, 0, 2$  mm) and a constant indentation load of 2.5 kN. The positive horizontal distance from the crack tip (i.e.  $H = 2$  mm) for double and triple indentations, resulted in higher life extension, and also influenced larger distance ahead of the crack tip by compressive residual stresses. Within the cases studied in this paper, triple indentations ahead of the crack tip provided higher FCG life improvements (435%) compared to both single (143%) and double (265%) indentation methods.

## References

- [1] Mendez, P. F. and Eagar, T. W. (2003) Penetration and Defect Formation in High-Current Arc Welding. *Weld J.* 82(10), 296-306.
- [2] Liu, C., Northwood, D. O. and Bhole, S. D. (2004) Tensile fracture behavior in CO<sub>2</sub> laser beam welds of 7075-T6 aluminum alloy. *Mater. Des.* 25, 573–577.
- [3] Elber, W. (1970) Fatigue Crack Closure under Cyclic Tension. *Eng. Fract. Mech.* 2, 37-45.
- [4] Sharp, P. K., Clayton, J. Q. and Clark, G. (1997) Retardation and Repair of Fatigue Cracks by Adhesive Infiltration. *Fatigue Fract. Eng. Mater. Struct.* 20(4), 605-614.
- [5] Shin, C. S. and Cai, C. Q. (2000) A model for evaluating the effect of fatigue crack repair by the infiltration method. *Fatigue Fract. Eng. Mater. Struct.* 23, 835–845.
- [6] Ayatollahi, M. R. and Hashemi, R. (2007) Mixed mode fracture in an inclined center crack repaired by composite patching. *Compos. Struct.* 81, 264-273.
- [7] Ayatollahi, M.R., Razavi, S.M.J. and Chamani, H.R. (2014) A numerical study on the effect of symmetric crack flank holes on fatigue life extension of a SENT specimen. *Fatigue Fract. Eng. Mater. Struct.* 37(10), 1153-1164.
- [8] Ayatollahi, M.R., Razavi, S.M.J. and Chamani, H.R. (2014) Fatigue Life Extension by Crack Repair Using Stop-hole Technique under Pure Mode-I and Pure mode-II Loading Conditions. *Procedia Eng.* 74, 18–21.
- [9] Ayatollahi, M. R., Razavi, S.M.J. and Yahya, M.Y. (2015) Mixed mode fatigue crack initiation and growth in a CT specimen repaired by stop hole technique. *Eng. Fract. Mech.* 145, 115-127.
- [10] Ayatollahi, M.R., Razavi, S.M.J., Sommitsch, C. and Moser, C. (2017) Fatigue life extension by crack repair using double stop-hole technique, *Mater. Sci. Forum*, 879, 3-8.
- [11] Razavi, S.M.J., Ayatollahi, M.R., Sommitsch, C. and Moser, C. (In press) Retardation of fatigue crack growth in high strength steel S690 using a modified stop-hole technique, *Eng. Fract. Mech.*

- [12] Carlson, R. L., Kardomateas, G. A. and Bates P. R. (1991) The effects of overloads in fatigue crack growth. *Int. J. Fatigue* 13(6), 453-460.
- [13] Shin, C. S. and Hsu, S. H. (1993) On the mechanisms and behaviour of overload retardation in AISI 304 stainless steel. *Int. J. Fatigue* 15(3), 181-192.
- [14] Dawicke, D. S. (1997) Overload and Underload Effects on the Fatigue Crack Growth Behavior of the 2024-T3 Aluminium Alloy. NASA Contractor Report.
- [15] Fairand, B. P. and Clauer, A. H. (1976) Effect of water and paint coatings on the magnitude of laser-generated shocks. *Opt. Commun.* 18(4), 588-591.
- [16] Yang, J. M., Her, Y. C., Han, N. and Clauer, A. (2001) Laser shock peening on fatigue behavior of 2024-T3 Al alloy with fastener holes and stop holes. *Mater. Sci. Eng. A298*, 296–299.
- [17] Buchanan, D. J., Shepard, M. J. and John, R. (2011) Emerald Article: Retained residual stress profiles in a laser shock peened and shot-peened nickel base superalloy subject to thermal exposure. *Int. J. Struct. Integr.* 2(1), 34-41.
- [18] Wang, S., Li, Y., Yao, M. and Wang, R. (1998) Compressive residual stress introduced by shot peening. *J. Mater. Process Tech.* 73, 64–73.
- [19] Černý, I. (2011) Growth and retardation of physically short fatigue cracks in an aircraft Al-alloy after shot peening. *Procedia Eng.* 10, 3411–3416.
- [20] Liu, J. (2013) Numerical analysis for effects of shot peening on fatigue crack growth. *Int. J. Fatigue* 50, 101–108.
- [21] Ray, P. K., Verma, B. B. and Mohanthy, P. K. (2002) Spot Heating Induced Fatigue Crack Growth Retardation. *Int. J. Pres. Ves. Pip.* 79, 373-376.
- [22] Ray, P. K., Ray, P. K. and Verma, B. B. (2005) A study on spot heating induced fatigue crack growth retardation. *Fatigue Fract. Eng. Mater. Struct.* 28, 579-585.
- [23] Chen, B. D., Griffiths, J. R. and Lam, Y. C. (1993) The Effects of Simultaneous Overload and Spot Heating on Crack Growth Retardation in Fatigue. *Eng. Fract. Mech.* 44(4), 567-572.
- [24] Goto, M., Miyagawa, H. and Nisitan, H. (1996) Crack growth arresting property of a hole and brinell-type dimple, *Fatigue Fract. Eng. Mater. Struct.* 19(1), 34–49.
- [25] Ruzek, R., Pavlas, J. and Doubrava, R. (2012) Application of indentation as a retardation mechanism for fatigue crack growth, *Int. J. Fatigue* 37, 92–99.
- [26] Song, P. S. and Sheu, G. L. (2002) Retardation of fatigue crack propagation by indentation technique, *Int. J. Pres. Ves. Pip.* 79, 725–733.
- [27] Lim, W., Song, J. and Sankar, B. V. (2003) Effect of ring indentation on fatigue crack growth in an aluminum plate, *Int. J. Fatigue* 25(9-11), 1271–1277.

**Table 1.** Mechanical properties of the aluminum alloy 7075-T6.

Elastic modulus (GPa)	Poisson's ratio	Yield strength (MPa)	Ultimate strength (MPa)	Elongation (%)
71.7	0.33	448	637	11

**Table 2.** Details of fatigue tests on CT specimens repaired by single indentation at the crack tip.

Indentation load, $F_{ind}$ (kN)	Total FCG life cycles (standard deviation %)	FCG life improvement* (%)	Minimum FCG rate (mm/cycle)	FCG rate reduction** (%)
Plain specimen	86,162 (6%)	-	1.51E-04	-
1	114,174 (9%)	33	2.09E-05	86
1.75	144,128 (11%)	67	1.24E-05	91
2.5	209,658 (8%)	143	6.88E-06	95

\* (Total FCG life of repaired specimen - total FCG life of plain specimen) / total FCG life of plain specimen  $\times$  100.

\*\* (FCG rate of plain specimen – FCG rate of repaired specimen) / FCG rate of plain specimen  $\times$  100.

**Table 3.** Details of fatigue tests on CT specimens repaired by double indentation in different horizontal positions.

Horizontal position of indentation, $H$ (mm)	Total FCG life cycles (standard deviation %)	FCG life improvement* (%)	Minimum FCG rate (mm/cycle)	FCG rate reduction** (%)
Plain specimen	86,162 (6%)	-	1.51E-04	-
-2	117,982 (5%)	37	2.64E-05	83
0	229,658 (8%)	167	6.84E-06	95
2	314,271 (12%)	265	4.62E-06	97

\* (Total FCG life of repaired specimen - total FCG life of plain specimen) / total FCG life of plain specimen  $\times$  100.

\*\* (FCG rate of plain specimen – FCG rate of repaired specimen) / FCG rate of plain specimen  $\times$  100.

**Table 4.** Details of fatigue tests on CT specimens repaired by triple indentation method in different horizontal positions.

Horizontal position of indentation, $H$ (mm)	Total FCG life cycles (standard deviation %)	FCG life improvement* (%)	Minimum FCG rate (mm/cycle)	FCG rate reduction** (%)
Plain specimen	86,162 (6%)	-	1.51E-04	-
-2	217,641 (9%)	153	6.56E-06	95.7
0	244,734 (11%)	184	5.71E-06	96.2
2	461,094 (13%)	435	2.71E-06	98.2

\* (Total FCG life of repaired specimen - total FCG life of plain specimen) / total FCG life of plain specimen  $\times$  100.

\*\* (FCG rate of plain specimen – FCG rate of repaired specimen) / FCG rate of plain specimen  $\times$  100.

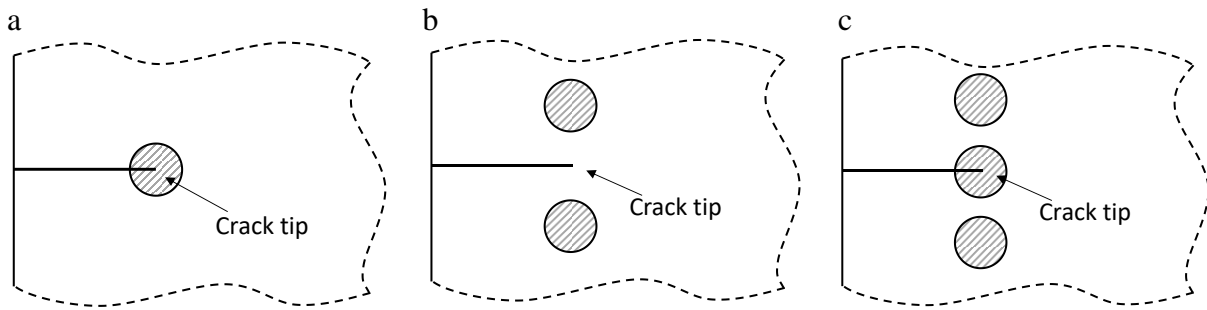


**Fig. 1.** Schematic view of (a) single indentation method, (b) double indentation method and (c) triple indentation method.

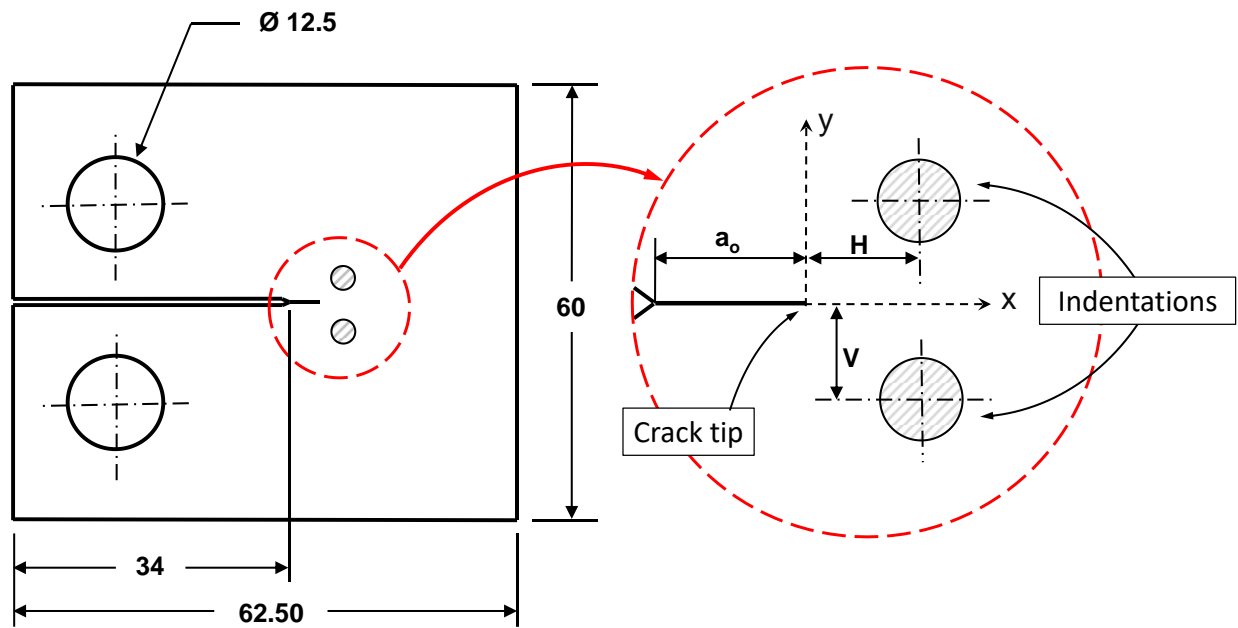


**Fig. 2.** Dimensions of CT specimen and indentation locations (dimensions in millimeters).



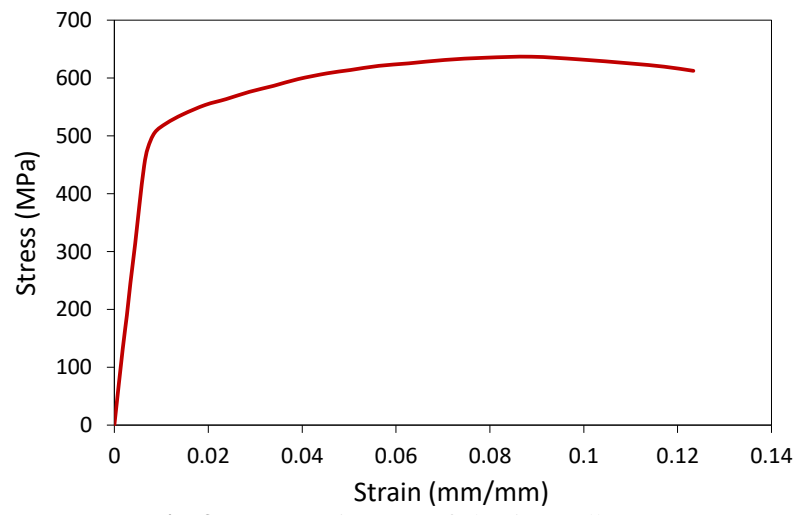


**Fig. 3.** Stress-strain curve of aluminum alloy 7075-T6.

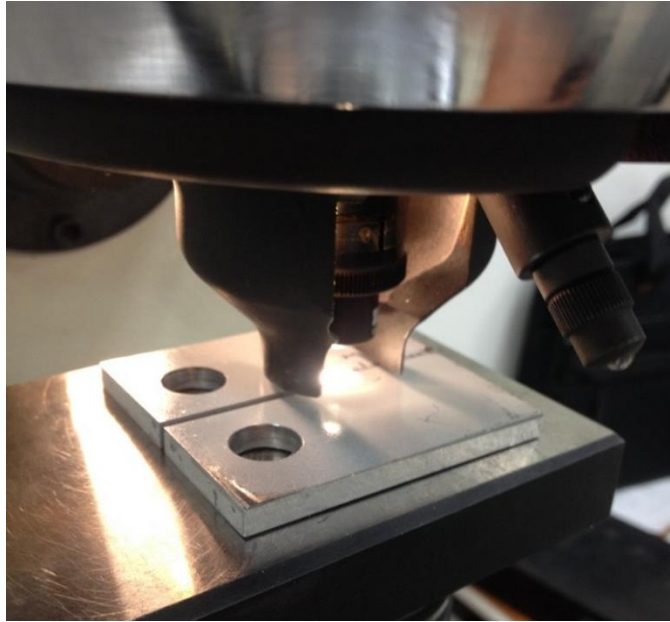


**Fig. 4.** Indentation configuration.

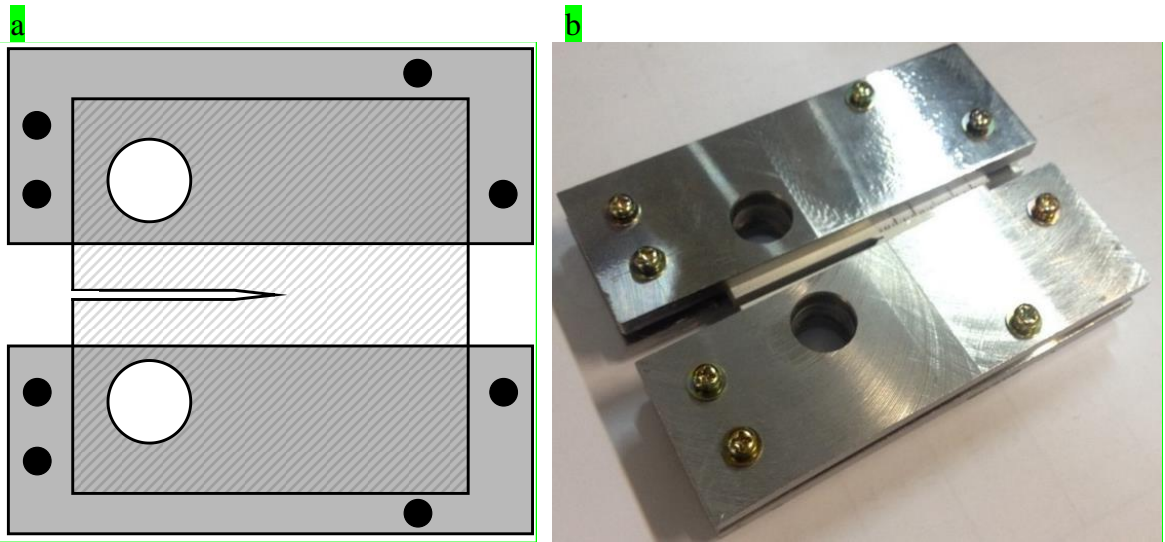


**Fig. 5.** Anti-buckling fixture on CT specimen (a) schematic view (b) experimental configuration



**Fig. 6.** Configuration of axial fatigue test used for testing CT specimens.

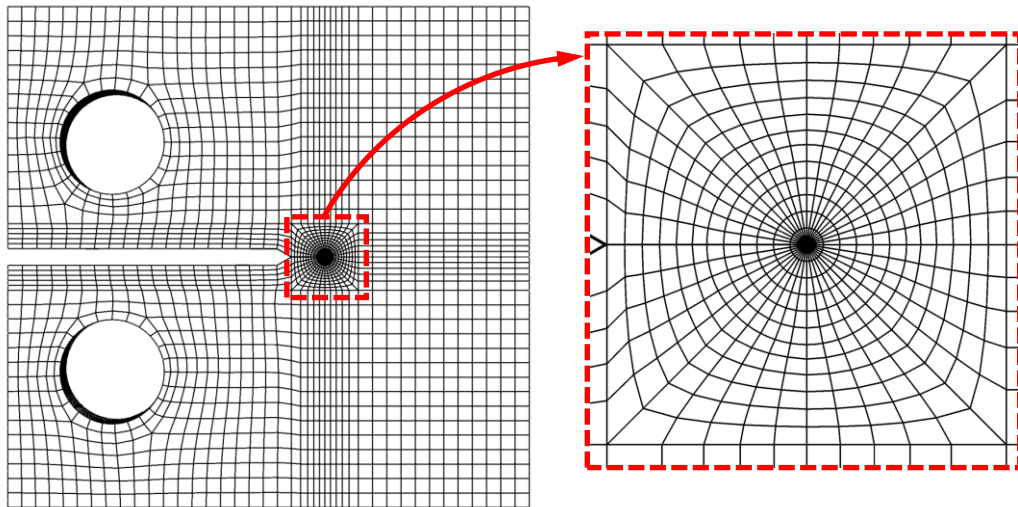


**Fig. 7.** FE model used for simulation of CT specimen.

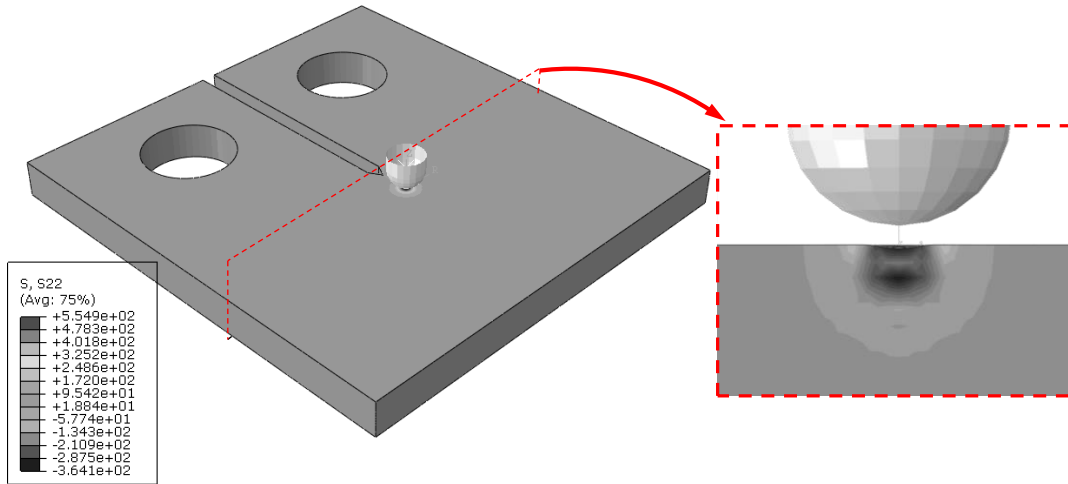


**Fig. 8.** Contour map of the residual stress through the thickness,  $\sigma_z$  near the crack tip (in MPa) induced by indentation load of  $F_{ind} = 1$  kN, before applying the opening force.

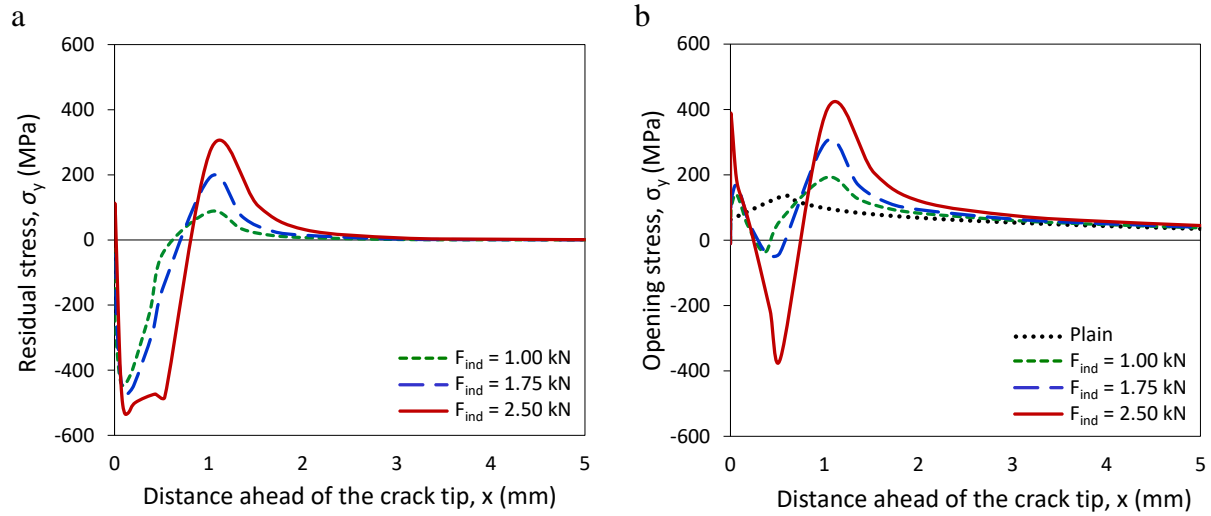


**Fig. 9.** Variations of  $\sigma_y$  for different indentation load levels of 2.5 kN, 1.75 kN and 1 kN;

(a) after indentation and before applying the opening force (residual stress) and (b) after applying opening force.

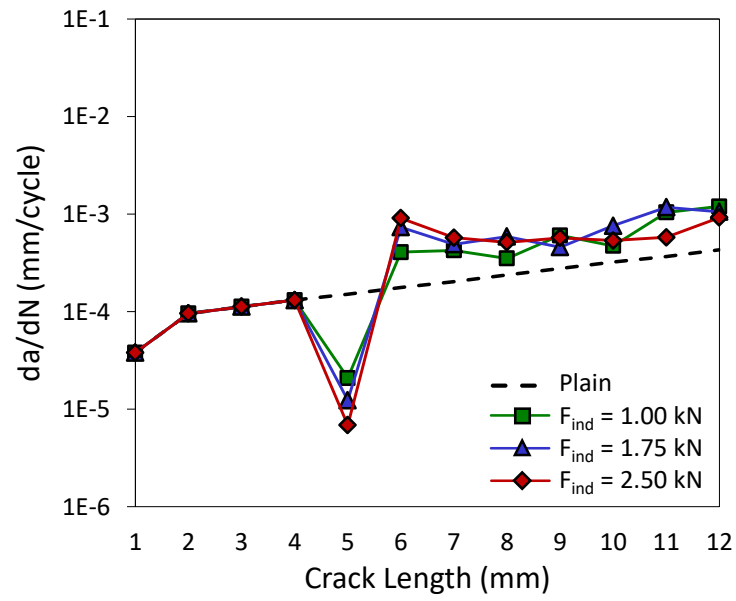


**Fig. 10.** FCG rate variation with respect to the crack length for different single indentation loads.



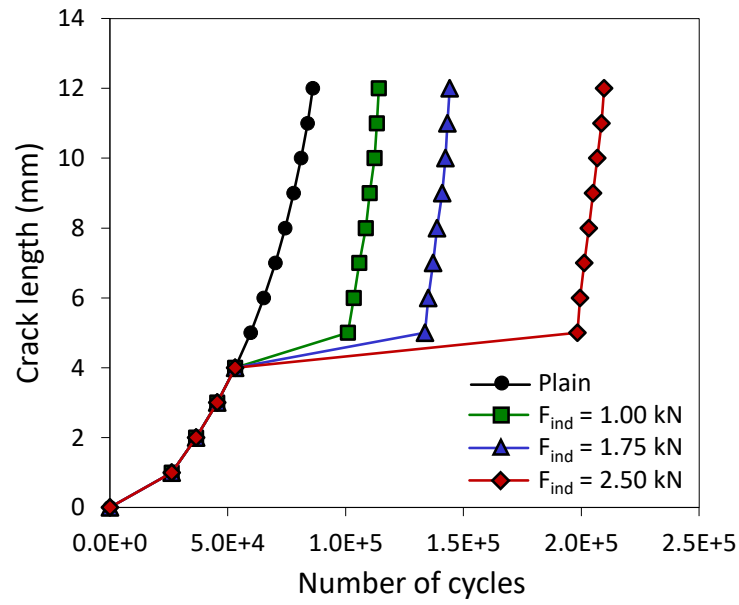
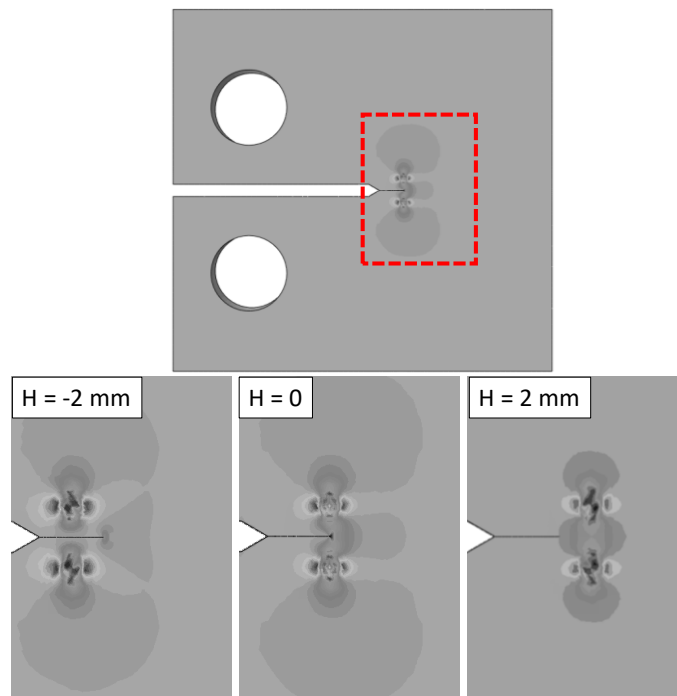
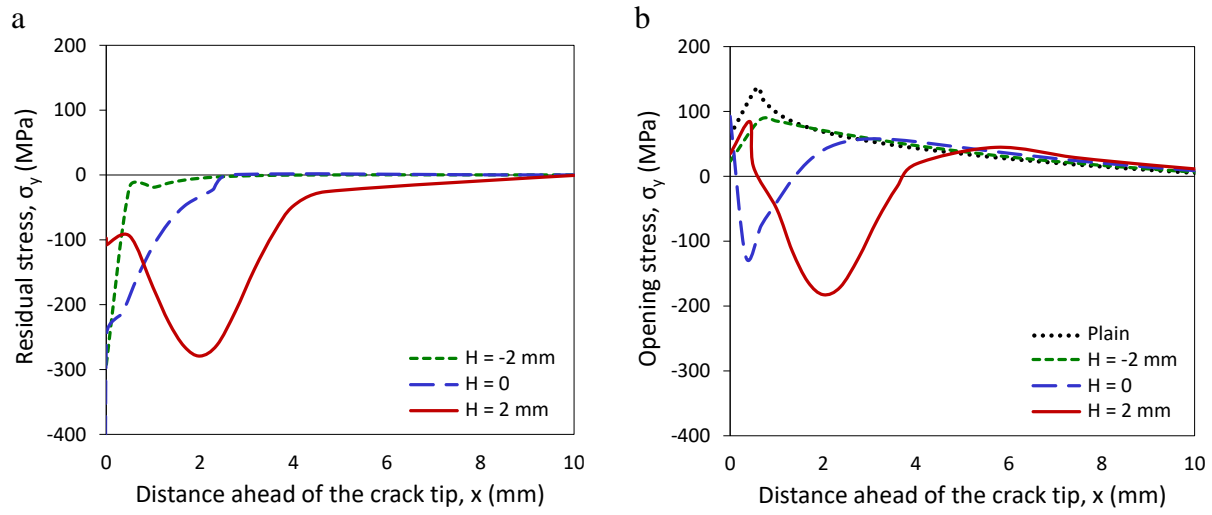


Fig. 11. Comparative FCG curves of specimens indented using 1 kN, 1.75 kN and 2.5 kN indentation load values.



**Fig. 12.** Distribution of residual stress,  $\sigma_y$  around the crack tip for double indented models with horizontal distances of (a)  $H = -2$  mm, (b)  $H = 0$  and (c)  $H = 2$  mm.



**Fig. 13.** Variations of  $\sigma_y$  for different horizontal distances  $H$  in double indentations ( $H = -2, 0$  and  $2$  mm); (a) after indentation and before applying the opening force (i.e. residual stress) and (b) after applying opening force.

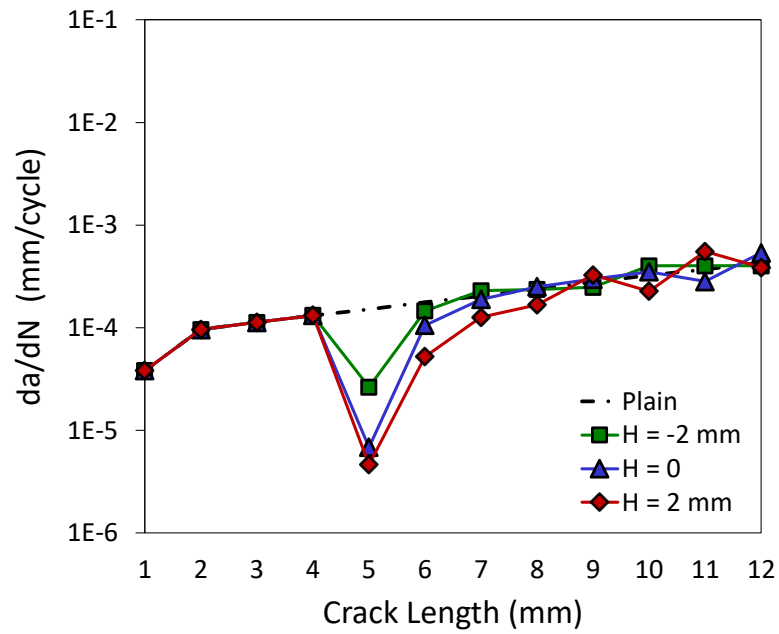


**Fig. 14.** FCG rate variation with respect to the crack length for different horizontal positions of double indentations.

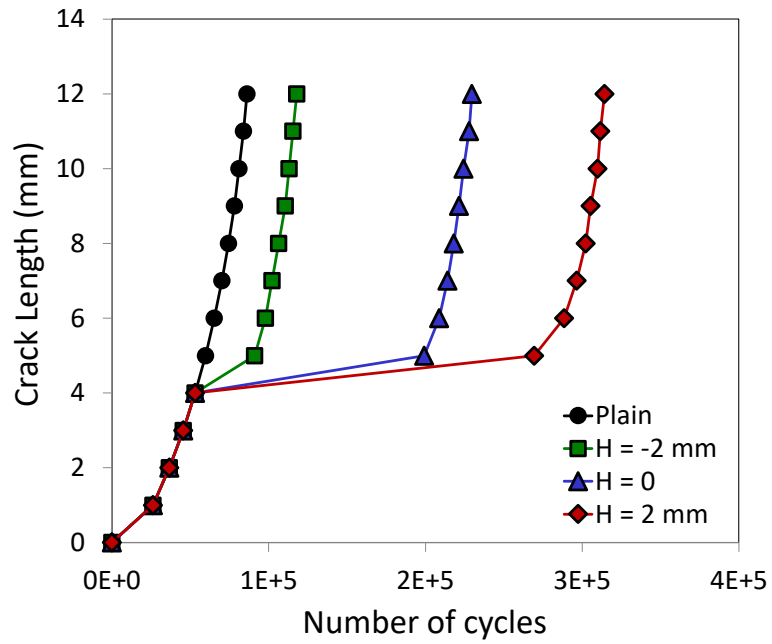


**Fig. 15.** Comparative fatigue crack propagation curves of double indented models in horizontal positions of  $H = -2$ , 0 and 2 mm.

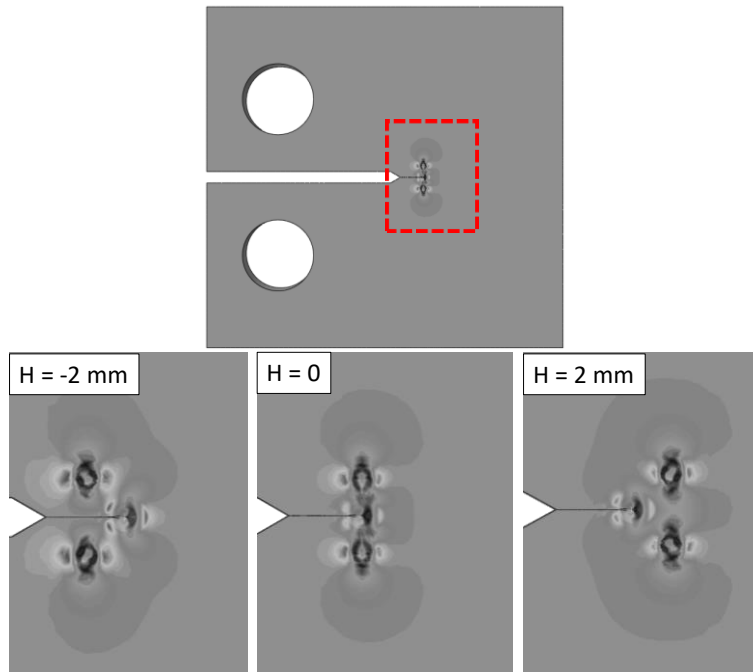


**Fig. 16.** Distribution of residual stress distribution,  $\sigma_y$  around the crack tip for triple indented models with horizontal distances of (a)  $H = -2$  mm, (b)  $H = 0$  and (c)  $H = 2$  mm.

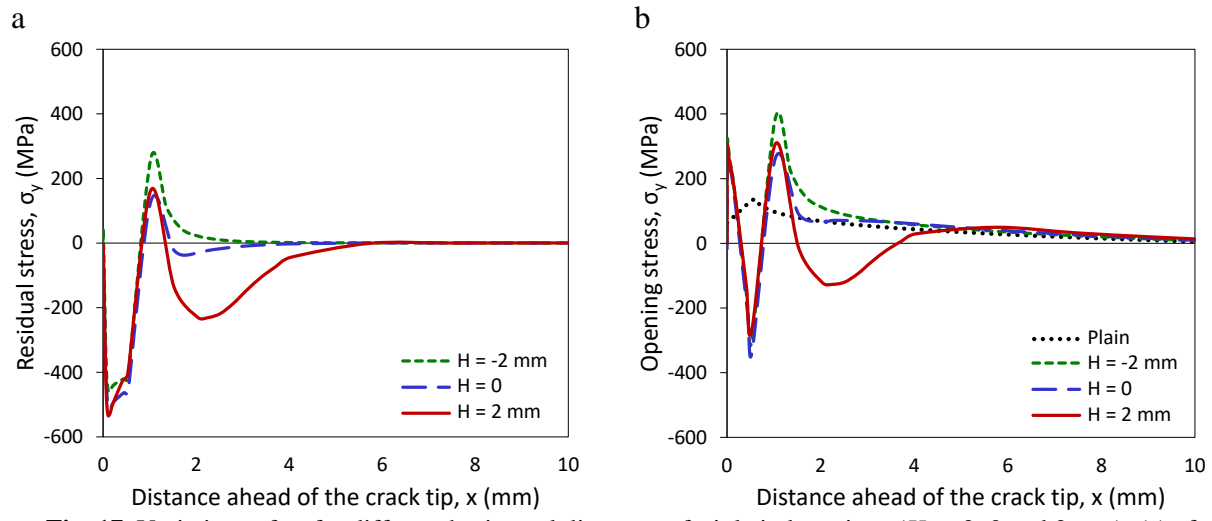


**Fig. 17.** Variations of  $\sigma_y$  for different horizontal distances of triple indentations ( $H = -2, 0$  and  $2$  mm); (a) after indentation and before applying the opening force (residual stress) and (b) after applying opening force.

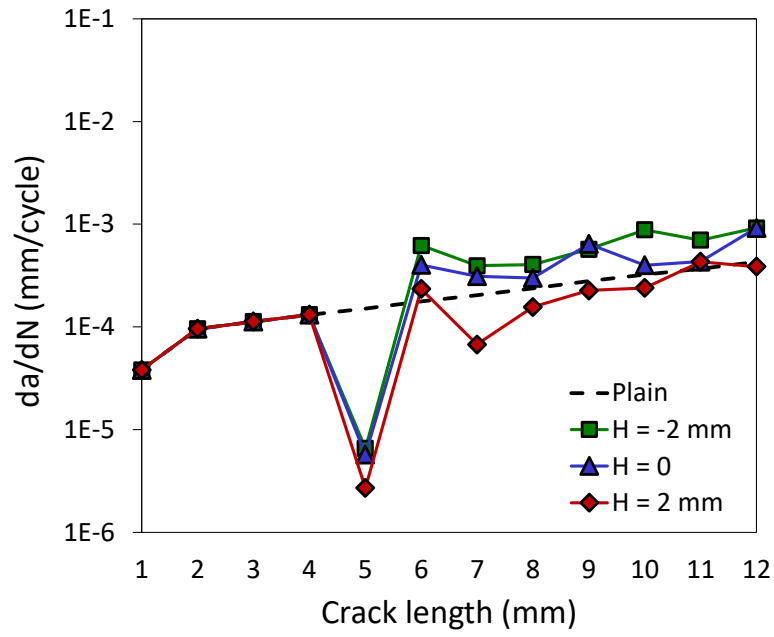


**Fig. 18.** FCG rate variation with respect to the crack length for different horizontal positions of triple indentations.



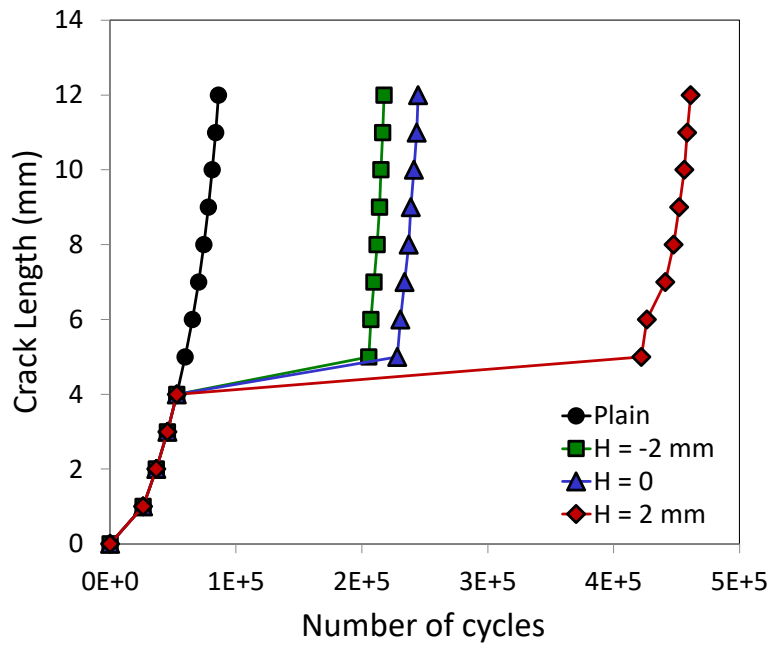


**Fig. 19.** Comparative fatigue crack propagation curves of triple indented models in horizontal positions of  $H = -2, 0$  and 2 mm.

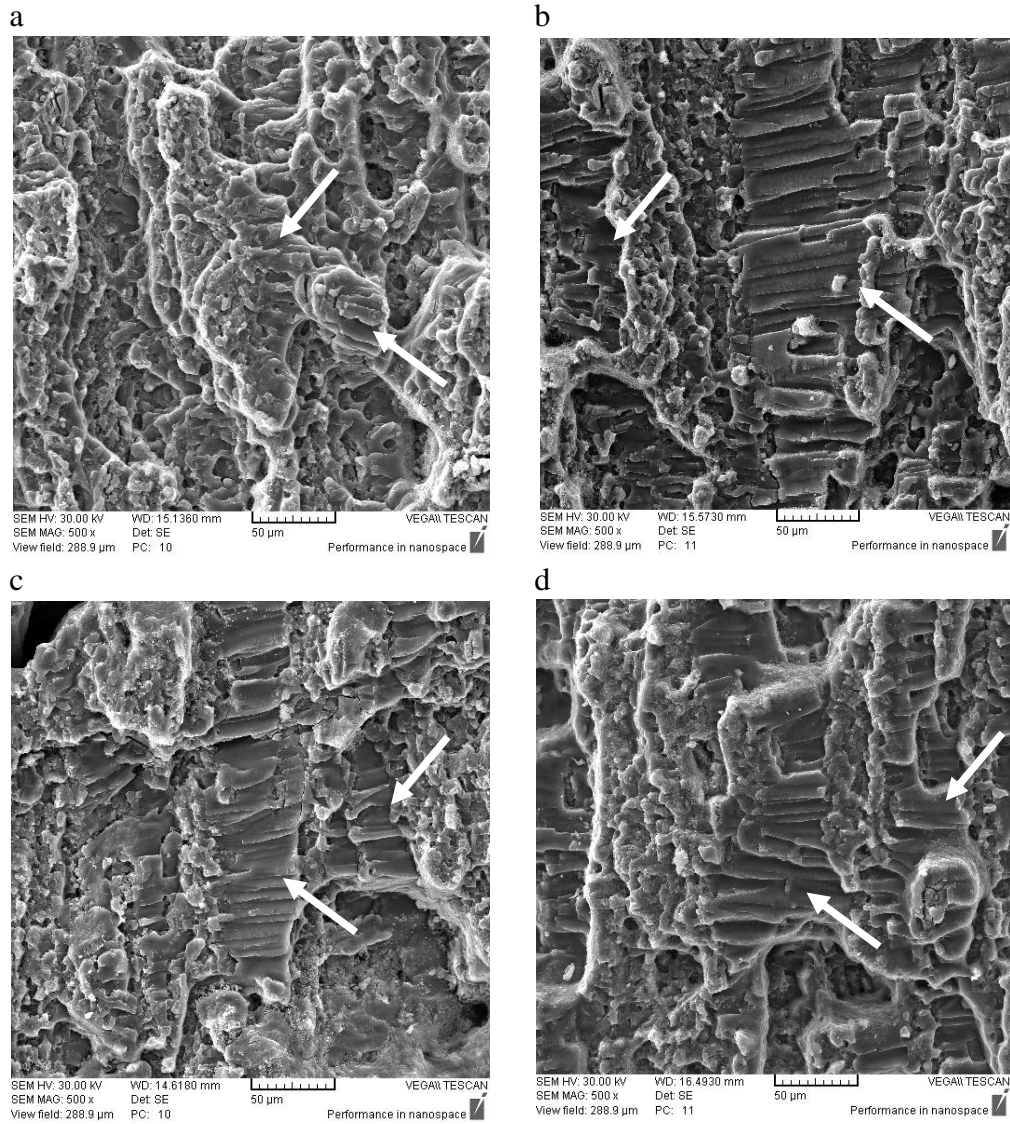


**Fig. 20.** The microscopic morphologies of fracture surface of test specimens; (a) plain specimen, (b) single indented specimen ( $F_{ind} = 2.5$  kN), (c) double indented specimen in horizontal position of  $H = 2$  mm ( $F_{ind} = 2.5$  kN), (d) triple indented specimens in horizontal position of  $H = 2$  mm ( $F_{ind} = 2.5$  kN).

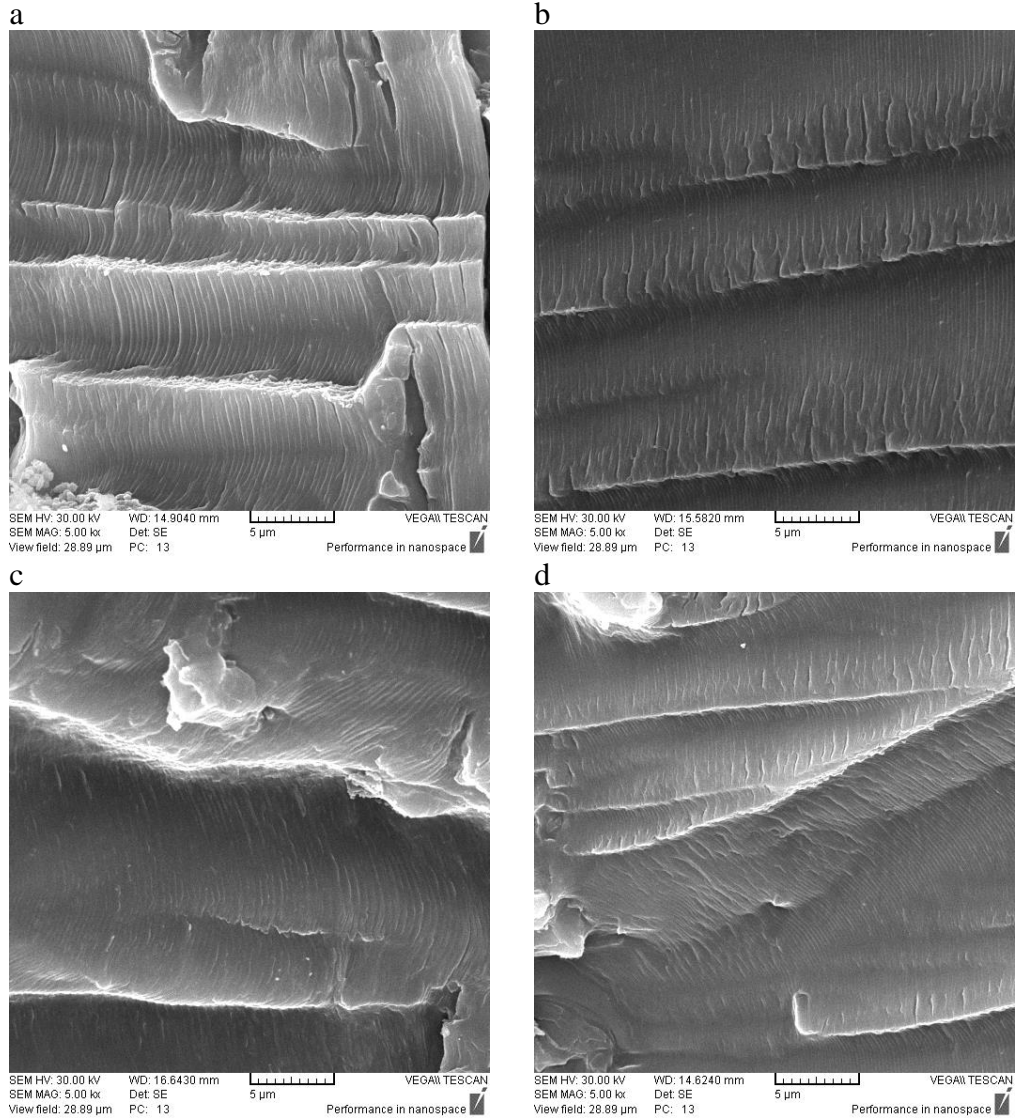


**Fig. 21.** The micro-morphologies of stable crack growth zone on test specimens; (a) plain specimen, (b) tip indented specimen ( $F_{ind} = 2.5$  kN), (c) double indented specimen in horizontal position of  $H = 2$  mm ( $F_{ind} = 2.5$  kN), (d) triple indented specimens in horizontal position of  $H = 2$  mm ( $F_{ind} = 2.5$  kN).